Morphology and Mechanical Properties of Polypropylene and Poly(ethylene-*co*-methyl acrylate) Blends

A. Genovese, R. A. Shanks

Department of Applied Chemistry, RMIT University, G.P.O. Box 2476V, Melbourne, Victoria 3001, Australia

Received 22 October 2002; accepted 1 January 2003

ABSTRACT: The morphology and mechanical properties of isotactic polypropylene (iPP) and poly(ethylene-*co*-methyl acrylate) (EMA) blends were investigated. Various EMA copolymers with different methyl acrylate (MA) comonomer content were used. iPP and EMA formed immiscible blends over the composition range studied. The crystallization and melting reflected that of the individual components and the crystallinity was not greatly affected. The size of the iPP crystals was larger in the blends than those of pure iPP, indicating that EMA may have reduced the nucleation density of the iPP; however, the growth rate of the iPP crystals was found to remain constant. The tensile elongation at break was greatly increased by the presence of EMA, although the modulus remained approximately constant until the EMA composition was greater than 20%. EMA with a 9.0% MA content provided the optimum effect on the mechanical properties of the blends. © 2003 Wiley Periodicals, Inc. J Appl Polym Sci 90: 175–185, 2003

Key words: poly(propylene) (PP); crystallization; mechanical properties

INTRODUCTION

Modification of isotactic polypropylene (iPP) properties is industrially important due to its wide applicability, functional usefulness, and low cost. Most often, this is achieved by the blending of iPP with another polymer or material. Of particular interest are blends of iPP with elastomers, owing to the wide range of engineering properties that they possess. Although PP has good abrasion and chemical resistance, and impermeability to water,[1,2] its drawback is its poor low-temperature impact behavior due to the relatively high glass transition temperature (T_g ~0°C). Therefore, the enhancement in the toughness of PP can be brought about by the inclusion of elastomer particles that dissipate mechanical energy through absorption and relaxation processes.

Studies of PP–elastomer copolymer systems often involve ethylene–propylene rubber (EPR),[3,4] ethylene–propylene–diene terpolymer (EPDM),[5] and styrene–ethylene–butylene–styrene (SEBS) block copolymers.[6,7] Other copolymers, such as poly(ethylene-*co*-vinyl acetate) (EVA) and poly(ethylene-*co*-methyl acrylate) (EMA), provide alternatives to conventional impact modifiers. Blends of PP and EVA, made by the crosslinking of the elastomeric phase with dicumyl peroxide, were investigated by Thomas et al.[8–10] The morphology of PP:EVA blends exhibits a two-phase structure where EVA is dispersed as domains when less than 50% of EVA is incorporated into the blend. The greater EVA content results in the formation of a cocontinuous phase morphology for a 30:70 blend. The crosslinking during mixing improved the mechanical properties; however, some degradation of PP was observed during the processing. PP blends with a noncrosslinked or crosslinked EVA and EMA phase were recently studied by De Loor et al.[1,11–13] These copolymers are completely miscible with each other and crosslinking was carried out *in situ* via a transesterification reaction during the extrusion process. This method permits stabilization of the particle-size morphology, which resulted in a uniformly dispersed phase. The impact strength is increased for blends containing a noncrosslinked EVA/EMA portion in PP:EVA/EMA blends with an increasing elastomeric phase. Cocontinuity of phases was observed for blends containing 40% or more elastomer, in conjunction with impact properties that remained constant thereon.[11] Crosslinking resulted in a more stable morphology, even during successive processing. An observed change in the morphology compared with a noncrosslinked blend of the same ratio and mixing history resulted in a larger elastomeric particle size due to breakup and coalescence phenomena.

Polymers which are toughened by blending often consist of a binary mixture of a minor phase dispersed in a matrix. The low entropy of mixing and weak interactions cause the components to be predomi-

Correspondence to: R. A. Shanks (robert.shanks@rmit.edu.au).

Journal of Applied Polymer Science, Vol. 90, 175–185 (2003)
© 2003 Wiley Periodicals, Inc.

TABLE I
Polymer Properties

Code[a]	Comonomer (wt %)	MFI (dg min^{-1})	Density (g cm^{-3})	T_c[b] (°C)	T_m[b] (°C)	ΔH_m (J g^{-1})	χ
PP	—	8.5	0.905	110.5	161.2	94.6	0.45
EMA6.5	6.5	6.0	0.928	84.0	99.4	102.3	0.34
EMA9.0	9.0	1.8–2.6	0.930	82.6	98.1	92.4	0.32
EMA16.5	16.5	0.7	0.938	69.3	85.8	66.8	0.23
EMA21.5	21.5	20.0	0.941	54.6	74.3	58.2	0.20

[a] All data were obtained from manufacturer technical literature.
[b]Crystallization and melting data obtained at a 10°C min^{-1} heating rate. All EMA curves display a shoulder on the lower-temperature side of the melting endotherm curve.

nantly immiscible as a result of differences in their physical and chemical structures and lack of specific interactions and polarity.[14] Toughening mechanisms depend on the elastomer particle size and adhesion to the matrix of the polymer system. Wu highlighted that, at a critical interparticle distance, a sharp transition from tough to brittle can be observed for polymer blends that are toughened through shear yielding of the matrix to dissipate energy.[15] The size and shape of the dispersed domains depend on the interfacial energy, polymer properties, and volume fraction of the blend components.

The polar EMAs are expected to be immiscible with iPP but they may modify the crystal structure of the surrounding iPP through changing the heterogeneous nucleation activity. PP and polyethylene (PE) copolymers have the same backbone structure; however, the side groups limit the miscibility of the two polymers under processing conditions. The composition, including the side group and content, morphology, and interfacial structure, govern the blend properties. PE domains usually form in an iPP matrix. The crystallization of iPP with the presence of different PEs results in a change of nucleation density. Blends containing low-density polyethylene (LDPE) resulted in a decrease in the number of nuclei as the content of LDPE increased. Galeski et al.[16] followed the migration of heterogeneous material from iPP to LDPE through the addition of a nucleating agent added to one of either of the components before blending. Other blends of iPP with random copolymers such as EPR or EPDM showed an increase in the nucleation density.[17] For blends containing high-density polyethylene (HDPE), heterogeneous material migrates away from iPP when crystallized above 127°C. Below this temperature, there is also migration away from iPP; however, the concentration of nuclei in the PE phase results in PE crystal growth that can nucleate iPP.[18]

In this research, we investigated the morphology and properties of the blends of iPP and EMAs of varying methyl acrylate (MA) content. As the MA content increases, EMA exhibits greater elasticity; however, it becomes less compatible with iPP due to the increased polarity. The use of polar toughening elastomers is expected to provide better adhesion properties at the surface and improved oil and hydrocarbon resistance. An added benefit of using EMA is that it possesses an excellent thermal stability compared with EVA, which decomposes through the loss of acetic acid[19] and can be used where better thermal properties are required.

EXPERIMENTAL

Materials

A commercial grade of iPP (Qenos Australia Pty Ltd., Melbourne, Australia) and four different EMA copolymers (Aldrich Chemical Co., Milwaukee, WI) with varying MA contents were used. Some polymer properties are listed in Table I.

Preparation of blends

iPP was blended with EMA at various composition ratios between 0 and 50 vol % EMA. The iPP:EMA blends were produced using an Axon BX-12 single-screw extruder (Axon Australia Pty. Ltd., Brisbane, Australia) equipped with a Gateway screw for polymeric dispersive mixing (12.5 mm diameter, *L:D* ratio of 26:1). The screw speed was 75 rpm and the operating temperatures were 140, 195, 198, and 190°C for feeding, metering, compression, and the die-end zone, respectively. The hot strands were rapidly cooled in water at 10°C prior to pelletization. All extruded pelleted samples were dried at 50°C for 12 h in a vacuum oven. Film specimens were prepared via a second extrusion by passing the molten blend through a 0.5 $\times$ 50-mm slit die and a chilled two-roller calendar.

Differential scanning calorimetry (DSC)

The crystallization (T_c) and melting (T_m) temperatures and enthalpies of crystallization (ΔH_c) and melting

(ΔH_m) of the samples were measured using a Perkin–Elmer DSC7 operating at ambient with an ice/water slurry as a coolant source. All experiments were conducted under a nitrogen purge with flow rate of 20 mL min^{-1}. The instrument was calibrated for temperature and enthalpy with high-purity indium (156.60°C, 28.45 J g^{-1}) and zinc (419.47°C, 108.37 J g^{-1}) standards. The calibration was periodically checked against the onset of melting for indium. Sample masses of ~2–3 mg cut from the films were accurately weighed using a Perkin–Elmer microbalance (AD-2Z autobalance) calibrated using standard milligram masses. The samples were encapsulated in standard hermetically sealed aluminum pans and a similar empty pan was used as a reference. The samples were held at 230°C for 5 min to eliminate the prior thermal history and self-seeding nuclei prior to cooling to 20°C at a rate of 10°C min^{-1}. A subsequent heating scan from 20 to 230°C at the same rate was performed. The degree of crystallinity, χ, was determined from eq. (1), where ΔH_m is the enthalpy of fusion, and ΔH_0, the enthalpy of pure crystalline PE (293 J g^{-1})[20] and PP (209 J g^{-1})[21]:

$$\chi = \frac{\Delta H_m}{\Delta H_0} \quad (1)$$

Mechanical and morphological properties

The mechanical properties were determined using an Instron universal testing instrument (Model 4465) at ambient temperature. Test specimens were cut from the extruded film into dumbbell-shaped test bars according to ASTM D638-97, specimen type IV. Each sample was placed under a strain rate of 50 mm min^{-1}. Measurements were taken on seven samples with the 95% confidence interval calculated and indicated on the graphs.

The crystallization growth rate was studied using hot-stage optical microscopy (HSOM). Specimens of 50-μm thickness were placed on a glass slide and held in place with a coverslip. The sample was placed on an FP90 Mettler hot stage and temperature-programmed using an FP82 Mettler central processor. The sample was heated to 230°C and held for 5 min to remove the thermal history prior to cooling to an isothermal crystallization temperature of 125°C. A Nikon Labophot II microscope with analyzing polarizers and a Sony CCD camera adapter was used. Images were captured and processed using an IP Lab Spectrum version 3.1a (Signal Analytics Corp.).

Scanning electron microscopy (SEM) was employed to obtain electron micrographs of film specimens using a Philips XL-30 SEM, with an accelerating voltage of 15–20 kV and a secondary electron detector. Specimens were prepared by cryogenically fracturing perpendicular to the direction of extrusion. Each specimen was sputter-coated with a conductive gold layer, applied for 10 s with 20-s intervals for a total time of 60 s, aimed at reducing localized heating of the low-melting EMA copolymer.

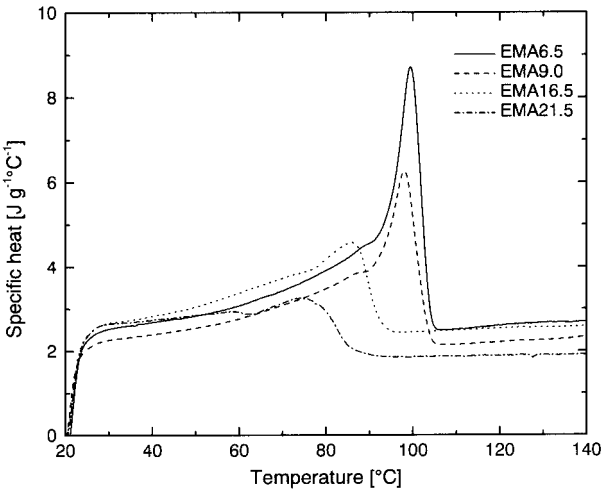

Figure 1 Specific heat melting curves for EMA copolymers with different MA content.

RESULTS AND DISCUSSION

Thermal properties of EMA

The melting specific heat curves for EMA copolymers with varying MA contents are displayed in Figure 1. The copolymers EMA6.5 and EMA9.0 have a relatively sharp main melting endotherm, whereas EMA16.5 and EMA21.0 exhibit broader melting endotherms, indicating the presence of a broader distribution of crystal morphologies. All EMAs show a broad shoulder on the lower-temperature side of the endotherm. EMAs are produced by copolymerization of ethylene and MA under high-pressure free-radical polymerization processes and they contain short-chain branches as a result of the insertion of MA units.[22–24] The distribution of MA co-units along the polymer chain is dependent upon the monomers' reactivity at the temperature and pressure of the polymerization process. Hence, a greater distribution (broad melting range) is seen for EMAs with higher MA contents.

The melting peak temperatures (T_m) of the copolymers are shown in Table I. It is observed that the T_m decreased linearly with an increasing MA content. The crystallization peak temperatures (T_c) are also given and follow a similar trend, whereas increasing the MA content shifts T_c to lower temperatures. The degree of crystallinity, χ, of the EMA copolymers was calculated according to Flory's theory of crystallization in copolymers where ethylene sequences are capable of crystallization and MA co-units are excluded from the

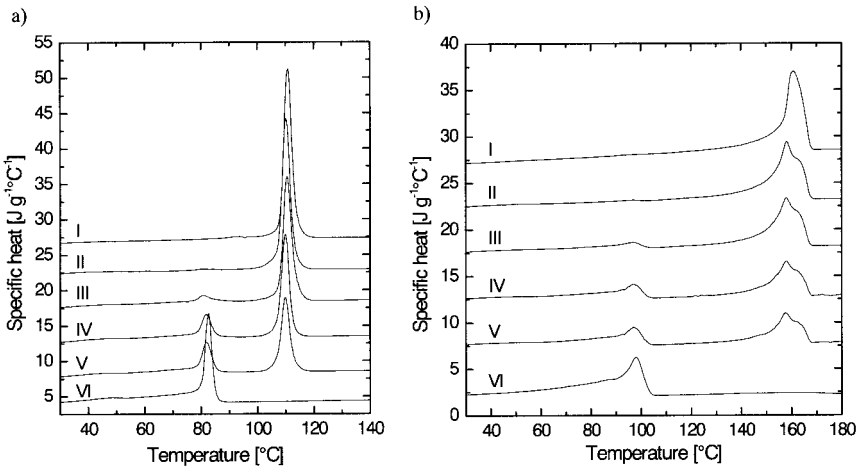

Figure 2 Specific heat curves for iPP:EMA9.0 blends and individual components: (a) crystallization and (b) melting curves. An incremental spacing of 5 units was added consecutively to each curve for clarity: (I) pure iPP; (II) 95:05; (III) 80:20; (IV) 60:40; (V) 50:50; (VI) EMA9.0.

crystal structure.[25] The degree of crystallinity of the EMA copolymers decreased with an increasing MA content from 0.34 for EMA6.5 to 0.20 for EMA21.5, which is the most elastomeric polymer. Similar findings were reported by Brogly et al.[26] for EVA copolymers with varying vinyl acetate (VA) content. The crystal structure is very sensitive to the amount of branching and crystallizable ethylene sequences, as observed for the EMA copolymers. Furthermore, they showed that EVA with less than 30% VA content obeyed the Flory and Burfield theory of copolymer crystallization, even though EVA is a multiphase material containing predominantly amorphous phases.

Thermal properties of iPP:EMA blends

The crystallization and melting specific heat curves for iPP:EMA9.0 blends are presented in Figure 2(a,b), respectively. The crystallization curves of pure iPP (curve I) and blends (curves II–V) display narrow exotherms, which are proportional to the blend composition. The EMA9.0 crystallization peak in the blends also exhibits a relatively sharp peak that is more prominent at higher proportions. The onset temperatures of crystallization [$T_{c(\text{onset})}$] for iPP and all the blends remained relatively constant at 113°C (Table II). Since no significant change in the $T_{c(\text{onset})}$ or T_c was detected, iPP is not nucleated by the presence of EMA. The width at half-height, an indication of the crystal population, showed less than a 0.3°C difference for the blends. The onset of crystallization of pure EMA9.0 and in the blends was observed to be very similar at about 85.0 and ~85.4°C, respectively. The crystallization peak temperature (T_c) of EMA9.0 was shifted by less than 2°C to lower temperature when the EMA content was increased in the blend.

The corresponding melting curves of the blends, shown in Figure 2(b), indicate separate melting peaks of the individual polymers. Pure iPP displays a single peak; however, the addition of EMA caused broaden-

TABLE II
Thermal Properties of iPP:EMA Blends

Code	T_m PP (°C)	ΔH_m PP (J g^{-1})	$T_{c(\text{onset})}$ PP (°C)	T_c PP (°C)	ΔH_c PP (J g^{-1})	χ	T_m EMA (°C)	ΔH_m EMA (J g^{-1})	T_c EMA (°C)	ΔH_c EMA (J g^{-1})
95% EMA6.5	158.4	76.8	114.4	110.6	−88.1	0.37	98.2	0.6	—	—
80% EMA6.5	158.2	63.0	113.7	109.6	−73.7	0.38	98.5	7.5	83.3	−7.7
60% EMA6.5	158.8	48.6	113.0	109.6	−56.1	0.39	99.4	17.8	84.1	−15.5
50% EMA6.5	158.0	39.9	112.7	109.6	−45.7	0.38	99.2	30.2	83.9	−45.9
95% EMA9.0	158.3	76.9	113.0	109.8	−85.9	0.39	—	—	—	—
80% EMA9.0	158.2	70.1	113.6	110.3	−73.5	0.42	96.5	4.9	80.8	−5.6
60% EMA9.0	158.0	49.2	112.6	109.6	−55.0	0.39	96.9	17.1	81.8	−35.5
50% EMA9.0	157.9	38.1	112.9	109.8	−45.8	0.36	97.5	26.5	81.8	−39.3
95% EMA16.5	158.4	76.6	113.0	110.1	−87.3	0.39	—	—	—	—
80% EMA16.5	157.4	64.2	113.3	110.3	−73.9	0.38	84.0	12.2	66.9	−10.7
60% EMA16.5	159.0	49.4	114.3	109.5	−57.3	0.39	87.2	20.5	68.6	−23.8
50% EMA16.5	158.0	39.9	112.6	109.6	−47.5	0.38	86.4	38.5	68.9	−28.2

ing of the iPP melting peak in the blends. The presence of a multiple endotherm observed in the blends indicates the formation of a disrupted and less perfect iPP crystal population. The peak at higher temperature is the result of the melting of rearranged iPP crystals on heating to higher melting crystals, which contain a greater degree of perfection, as suggested by Kim et al.[27] As a consequence of an increasing copolymer content, the relative amount of rearranged crystals, indicated by the area of the endotherm, also proportionally increased. The degree of crystallinity for iPP was decreased from 0.45 (pure) to 0.39 for the 95:05 iPP:EMA blend. Further EMA additions, in general, resulted in little change in the crystallinity. Similar results were obtained for blends of iPP:EMA6.5 and iPP:EMA16.5 as indicated in Table II. Danesi and Porter similarly reported, for immiscible blends of PP: EPR, that the melting temperature and enthalpy of fusion of PP had only been marginally affected by the presence of the rubber and the crystallization was essentially found to be independent of the rubber content.[4]

Morphology of iPP:EMA blends

Polarized optical micrographs of thin films of pure iPP and iPP:EMA6.5 blends are shown in Figure 3. The films were held at 230°C for 5 min to remove traces of crystallinity prior to isothermal crystallization at 125°C. The microstructures of pure iPP and the blends show marked changes with the variation of the EMA6.5 composition. The spherulitic structure of iPP is evident, particularly in the blends where the α-modification is clearly seen. However, the size of the crystals of pure iPP was relatively small and the incorporation of EMA6.5 resulted in an increase in the size of the spherulites. The addition of 5% EMA caused the formation of larger and distinct iPP spherulites with defined boundaries [Fig. 3(b)]. This is believed to be a result of the polarity of the EMA that may extract nuclei from the iPP matrix. While iPP spherulites form, the EMA is repelled from the growth front and accumulates in the interspherulitic regions. For the blends of ratios 85:15 to 50:50, the iPP spherulites were found to decrease in size. Therefore, as the EMA content increased, it inhibited the growth of larger crystallites, imposing physical limitations on molten iPP migrating to the growing spherulite front, in conjunction with high nucleation rates. The growth rate of iPP in the blends, determined by measuring the radius of the spherulites over time before impingement, was similar for all the compositions. Hence, the influence of EMA on the iPP morphology is evident, although the degree of crystallinity of the iPP remained relatively unchanged, as previously observed from the DSC measurements.

SEM observations of the fractured surfaces of iPP blends with EMA6.5 and EMA9.0 are shown in Figures 4 and 5, respectively. Figure 4(a) displays a characteristically brittle fracture surface of iPP, evidence of its inherent crystallinity. The blends all show a two-phase morphology with EMA distinctly visible as separate domains in the iPP matrix, clearly showing the immiscibility of the blend components. For these blends, EMA formed the minor phase, including that of the 50:50 blend ratio. No evidence of cocontinuity was observed for the blends studied. As the content of EMA6.5 was increased to 20%, the copolymer displayed elongated droplets in the direction of extrusion. The particles are less than 1 micron in diameter and are uniformly dispersed in the iPP matrix. This is evident in Figure 4(c), wherein the bulk of the material shows uniformity of the EMA dispersed phase. The 75:25 blend shows dispersed EMA; however, the domains are not as uniform in size and distribution, leading to a morphology where the domains become more continuous. The lack of interfacial adhesion exhibited by all blends also indicates that the polar EMA at a high-volume content will result in reduced mechanical properties. Similar morphologies were observed for blends of iPP:EVA[8] and blends of LLDPE: EMA,[28] where the two phases were found to be immiscible at all compositions. For blends containing EMA9.0, the fractured surface of the blend ratio of 95:05 (Fig. 5) shows a more ductile appearance, with voids where EMA droplets were present. A lack of interfacial adhesion can be seen between the phases. This is also observed for all the compositions of the iPP:EMA9.0 blends. Nonetheless, the distribution of EMA9.0 is not as uniform as that seen for EMA6.5 blends and the particle size is more variable with droplets to 4 μm. The evidence of ductility can be observed for blend ratios containing more than a 20% copolymer content with elongated EMA fibrils.

Mechanical properties of iPP:EMA blends

The tensile tests of all the samples displayed typical characteristics of a ductile thermoplastic. Stress whitening occurred almost instantaneously followed by drawing with the applied strain. The tensile strain at break as a function of the composition is shown in Figure 6. Almost all the blends showed an increase in the strain at break. PP more than doubled in length and the addition of EMA contributed by enhancing the elongation of the specimens. In general, the strain at break increased to 80 vol % EMA before declining toward a 50 vol % composition. This is consistent with PP blended with the poly(ethylene-*co*-propylene) (EP) elastomer, where 20–30 vol % of the elastomer provided an optimum.[4] EMA is expected to be less compatible with PP than with EP due to the polarity of the

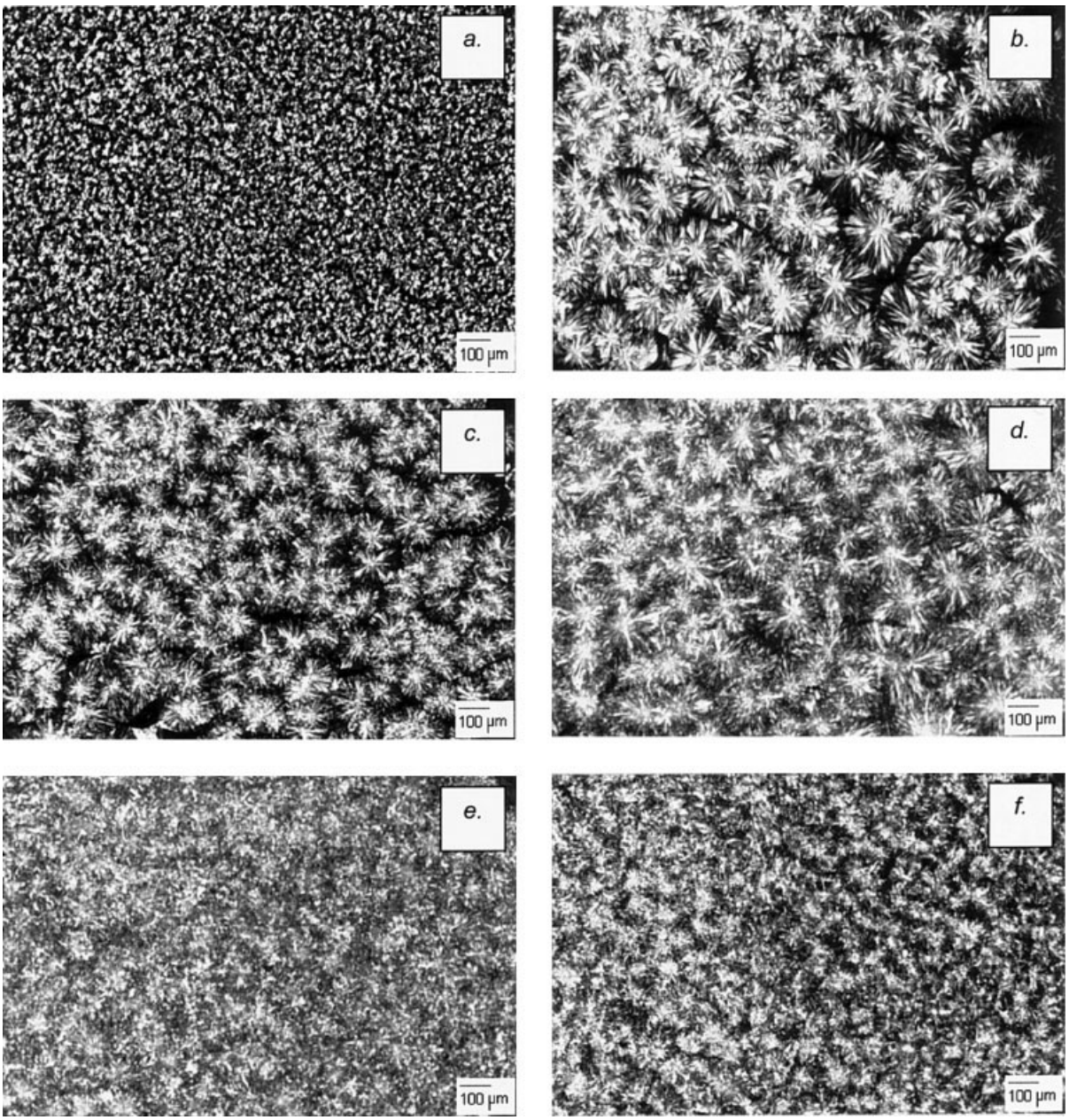

Figure 3 Photomicrographs of iPP:EMA6.5 blends: (a) pure iPP; (b) 90:10; (c) 85:15; (d) 75:25; (e) 50:50.

MA groups and lack of favorable specific interactions. The strain at break increased to a maximum at 9.0 or 16.5 wt % MA and then decreased, more so for the latter series. At the low level of 5 vol % EMA, the 16.5 wt % MA copolymer provided the maximum strain at break, but for the other blend compositions, 9.0 wt % provides the maximum overall. The maximum strain at break for all the compositions was 20 vol % EMA containing 9.0 wt % MA.

The strength of the blend is primarily that of iPP, which, in turn, depends on the crystallinity. Since the blends did not show significant changes in the degree of crystallinity, the crystal morphology as shown previously influences the properties of the blends. The EMA with an increasing MA content became more elastomeric, coinciding with an overall reduction in the crystallinity. The results suggest that a compromise is present between the increased elastomeric properties of EMA with a high MA content and decreased compatibility with increased polarity of the copolymer. An increasing MA content was shown to decrease the crystallinity of the copolymer and, hence, lower the pseudocrosslinks or the amount of tie molecules present in the EMA.[29] At a low concentration of EMA, that is, 5 vol %, the 16.5 wt % EMA can provide the highest strain at break, but as the concentration of

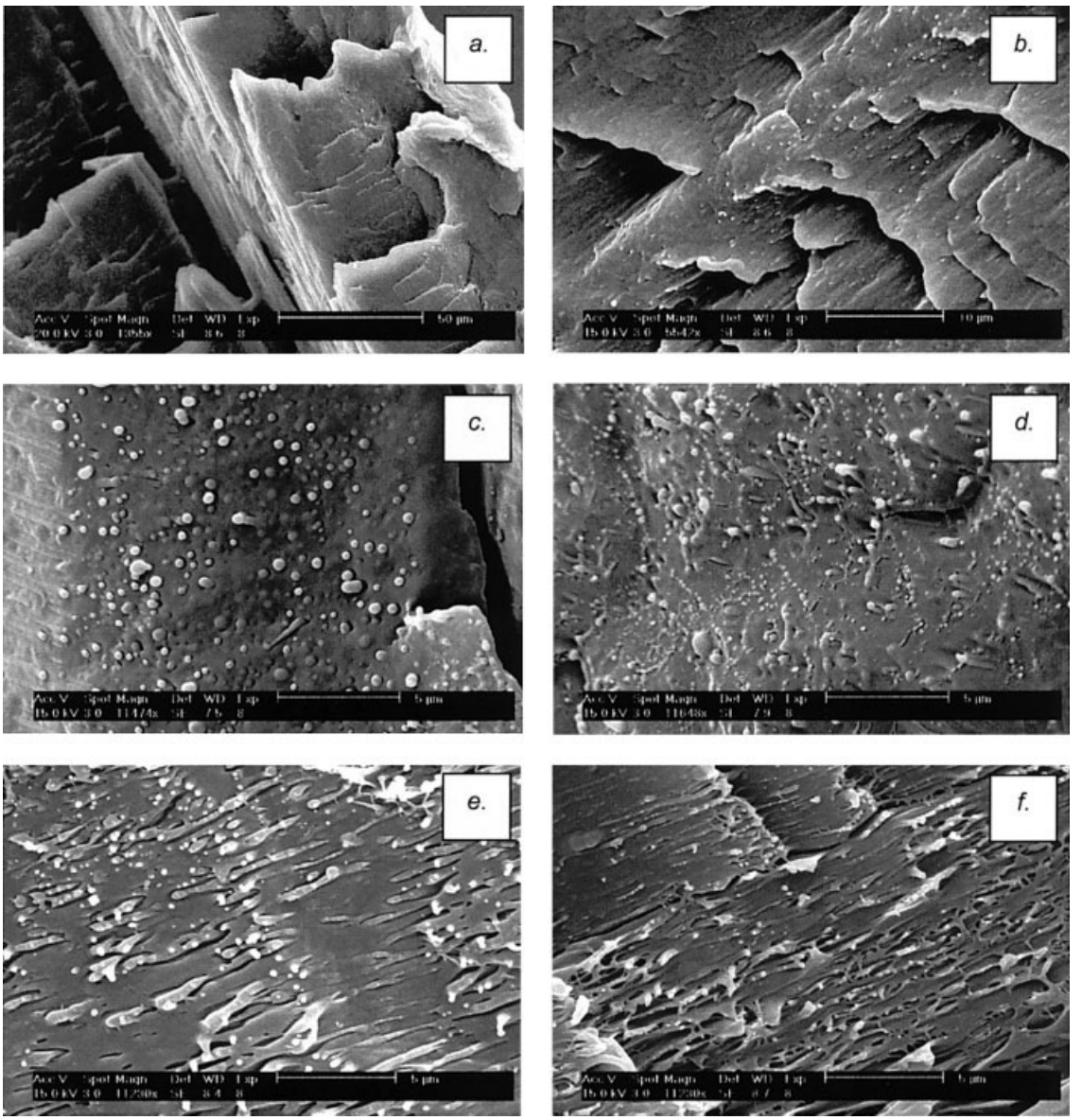

Figure 4 SEM images of iPP:EMA6.5 blends with varying EMA6.5 content: (a) pure iPP; (b) 95:05; (c) 80:20; (d) 75:25; (e) 60:40; (f) 50:50.

EMA increases, the compatibility between the components becomes more important. Consequently, 16.5 wt % EMA becomes less suitable and the 9.0 wt % EMA becomes the more dominant additive, contributing greater over the composition range. The 9.0 wt % EMA provided twice the strain at break of pure PP when present at 20 vol %. The absolute strain at break of 540% is a significant increase over that of pure PP, where a 250% strain at break was obtained.

The modulus for iPP:EMA blends is shown in Figure 7. The Young's modulus is progressively reduced by the addition of increasing proportions of EMA. The modulus of iPP cannot be enhanced through blending with an elastomer. The purpose when blending a hard polymer with an elastomer is to minimize the reduction in stiffness. The modulus of the blends does not decrease significantly below 1000 MPa until greater than 20 vol % of the elastomer has been included. This is important because 20 vol % EMA is the concentration where the greatest increase in strain at break was observed. At 75 vol % EMA, the modulus starts to decrease rapidly, and by 50 vol %, it has reached about 600 MPa and the system may be approaching phase inversion, whereby the EMA may become the continuous phase. The variation in the MA content of EMA did not produce consistent changes in the modulus. The EMA containing 21.5 wt % EMA caused a greater decrease in the modulus than did the other compositions at 20 and 25 vol % iPP. Other variations were within experimental uncertainty. The modulus is ex-

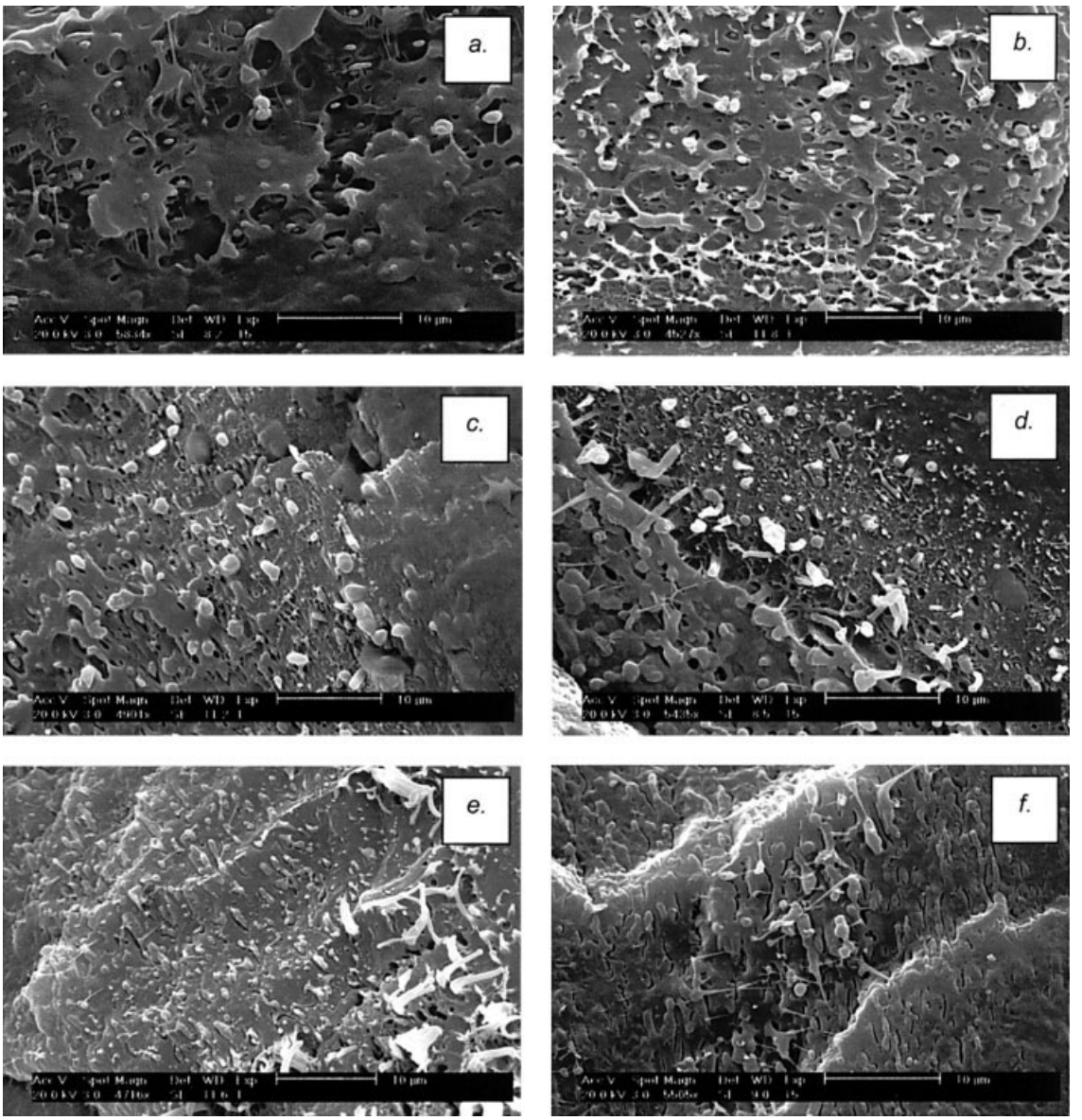

Figure 5 SEM images of iPP:EMA9.0 blends with varying EMA9.0 content: (a) 95:05 PP; (b) 90:10; (c) 80:20; (d) 75:25; (e) 60:40; (f) 50:50.

pected to be determined mainly by the continuous phase.

The yield stress is shown in Figure 8 for the various blends with changes in the composition and MA level in the EMA. In these results, the yield stress decreased significantly with the addition of only 5 vol % EMA. The exception to this was EMA6.5, where at 5 and 10 vol % the yield stress was not significantly changed from the pure iPP. Since EMA9.0 was the most suitable of the EMAs for the strain at break and modulus, this is the composition on which emphasis will be focused. The yield stress of iPP:EMA9.0 decreases rapidly from 33 to 26 MPa with the addition of 5 vol % EMA9.0. With addition of further amounts of EMA9.0, the yield stress values decrease continuously to about 18 MPa at 50 vol %. The composition of most interest is 20 vol % EMA9.0 and the yield stress was 22 MPa. The decrease is not consistent with the MA content of the EMA, other than for EMA6.5. EMA6.5 has the greatest crystallinity and so will be the least likely to yield. The other EMA copolymers are expected to yield more readily as the MA content increases. The stress on the iPP matrix must be transferred to the EMA droplets. If the interface is weakened with more polar EMA and the blend is less compatible, then the yield will decrease more rapidly. The continuous decrease in yield is the property that the iPP:EMA blends have decreased performance with the composition. These trends agree with those of the PP:EVA–EMA noncrosslinked elastomer phase by De Loor et al.[11]

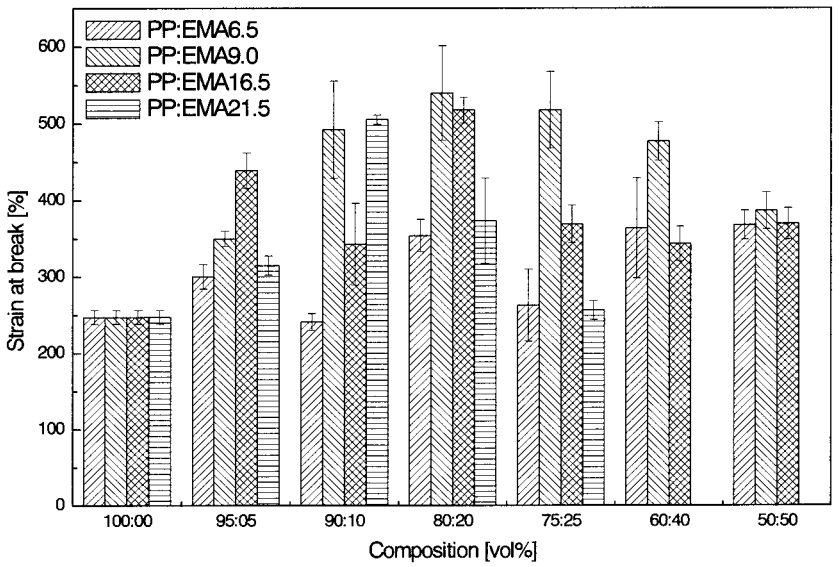

Figure 6 Strain at break for iPP:EMA blends with varying blend ratios and MA content.

Overall, the mechanical properties demonstrated that iPP can be toughened more effectively with a low EMA content.

Gupta et al.[30] investigated the impact strength of PP:EVA blends of various compositions and VA contents in EVA. They found that the blends containing EVA12.0 (12.0 wt % VA content) provided a reasonable improvement in the impact properties since they offered a good compromise over the composition range. Blends containing EVA19.0 (19.0 wt % VA content) showed less consistency in the results, which was attributed to the strongly interacting polar VA groups in the copolymer. These results support the current finding for the relative performances of the EMA copolymer.

The effect of blend composition has a marked influence on the mechanical properties. The importance of the MA content is also evident. EMA6.5 behaves closer to that of a thermoplastic due to a low MA content and higher crystallinity, resulting in lower elongation in the iPP:EMA6.5 blend system. A higher MA content increases the polarity of the ethylene copolymer and reduces the molecular compatibility between the blend components, along with increased elastomeric properties. Accordingly, EMA21.5 is inherently the most elastomeric, as can be seen by the vast improve-

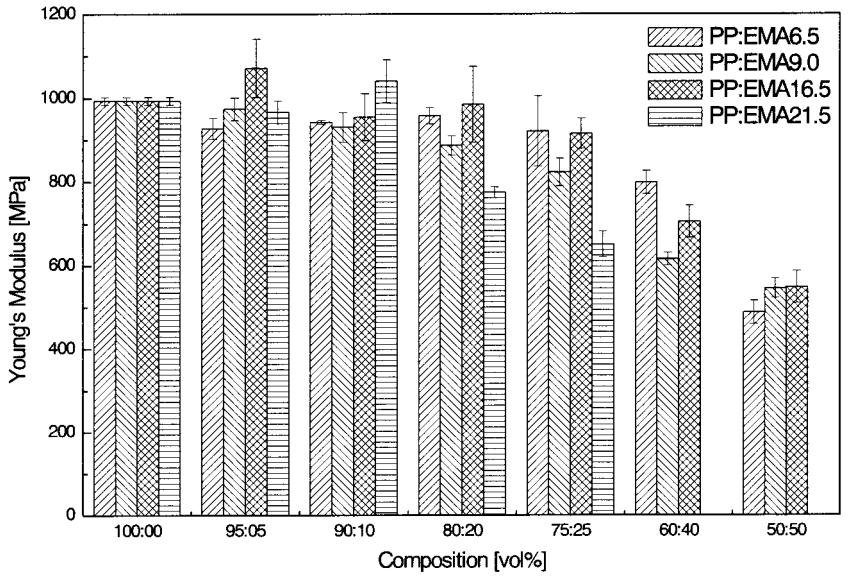

Figure 7 Modulus of elasticity (Young's modulus) for iPP:EMA blends with varying blend ratios and MA content.

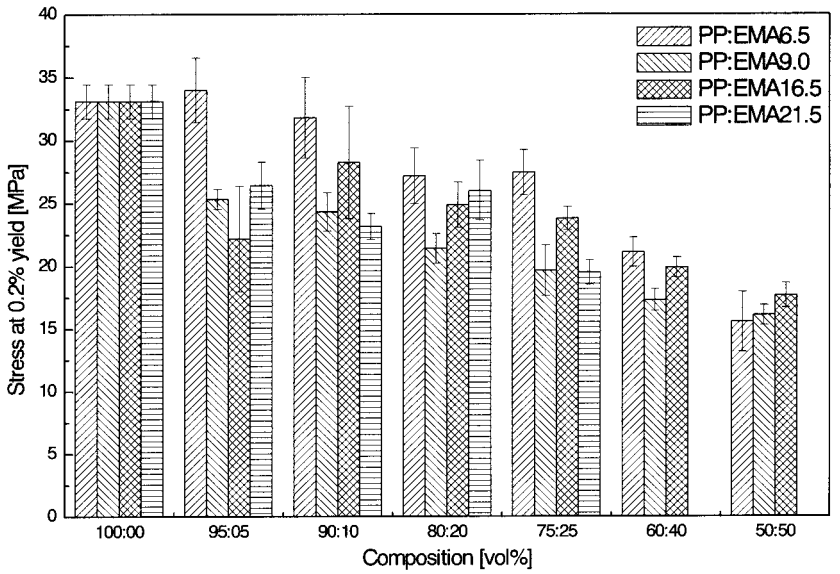

Figure 8 Yield stress for iPP:EMA blends with varying blend ratios and MA content.

ment in the 90:10 blend. However, a reduction in the strain at break compared to that of iPP itself suggests that an incompatibility due to the high polarity of EMA and a lack of specific interactions between components exist, thereby giving low interfacial adhesion. Similarly, EMA16.5 blends are elastic but too polar for sufficient interaction to maintain mechanical properties due to the high MA content. The optimal blend seems to be iPP:EMA9.0, where the properties were well maintained over the composition range studied. The addition of 10–25% EMA9.0 in an iPP matrix shows that the compatibility over this range provides an optimum between the elastomeric properties and the polarity of EMA. Studies of PP:EVA[10] and PP:EPDM[5] showed similar mechanical properties to those observed for the PP:EMA blends, allowing for differences between the types of PP. The following results were estimated for 70:30 blends of PP and the elastomer, with the values in brackets that of the pure PP: The modulus change, compared with pure PP for PP:EMA, 900 MPa (1000), was less than that for PP:EPDM, 800 MPa (1200). In addition, the yield stress was not reduced greatly at 22 MPa (33) from that of pure PP, compared with PP:EVA, 21 MPa (42), and PP:EPDM, 10 MPa (80). The elongation at break was lower since the PP used in the current study showed more extensional behavior, 500% (250), compared with PP:EVA, 101% (18), and PP:EPDM, 20 (5).

CONCLUSIONS

The morphology and tensile mechanical properties of iPP were modified by the incorporation of EMA copolymers of varying MA content. They are sufficiently compatible at a low MA concentration for the EMA to enhance the ductility of the blends without a severe loss in stiffness. The optimal tensile performance was obtained for a 80:20 blend ratio of iPP:EMA9.0, where the strain at break was increased 300%. EMA9.0 has the optimum elasticity-to-polarity ratio to increase the ductility. Increased MA content in the copolymer resulted in poor interfacial adhesion and, therefore, a reduction compatibility as seen for EMA16.5 and EMA21.5 blends, particularly with higher EMA content. A 20% content of EMA is similar to the content of other elastomers, such as EPR, EPDM or SEBS, where optimum toughness is obtained. This volume fraction in the range of 15–20% allows the elastomer particles to be separated by less than the critical ligament distance.

One of the authors (A. G.) acknowledges the receipt of an Australian Postgraduate Award (APA). Special thanks are given by the authors to Dr. Gandara Amarasinghe for suggestions in the preparation of this manuscript.

References

1. Dutra, R. C. L.; Soares, B. G.; Gorelova, M. M.; Silva, J. L. G.; Lourenço, V. L.; Ferreira, G. E. J Appl Polym Sci 1997, 66, 2243.
2. Walling, N.; Kamal, M. R. Adv Polym Technol 1996, 15, 269.
3. Starke, J. K.; Michler, G. H.; Grellmann, W.; Seidler, S.; Gahleitner, M.; Feibig, J.; Nezbedova, E. Polymer 1998, 39, 75.
4. Danesi, S.; Porter, R. S. Polymer 1978, 19, 448.
5. Hoppner, D.; Wendorff, J. H. Colloid Polym Sci 1990, 268, 500.
6. Gupta, A. K.; Purwar, S. N. J Appl Polym Sci 1984, 29, 1079.
7. Gupta, A. K.; Purwar, S. N. J Appl Polym Sci 1985, 30, 1777.
8. Thomas, S.; Gupta, B. R.; De, S. K. Kautsch Gummi Kunstst 1987, 40, 665.
9. Thomas, S.; Gupta, B. R.; De, S. K. J Mater Sci 1987, 22, 3209.
10. Thomas, S. Mater Lett 1987, 5, 360.

11. De Loor, A.; Cassagnau, P.; Michel, A.; Vergnes, B. J Appl Polym Sci 1997, 63, 1385.
12. De Loor, A.; Cassagnau, P.; Michel, A.; Vergnes, B. J Appl Polym Sci 1995, 53, 1675.
13. De Loor, A.; Cassagnau, P.; Michel, A.; Vergnes, B. Int Polym Process 1994, 9, 211.
14. Utracki, L. A. Polymer Alloys and Blends; Oxford University: New York, 1989.
15. Wu, S. Polymer 1985, 26, 1855.
16. Galeski, A.; Bartczak, Z.; Pracella, M. Polymer 1984, 25, 1323.
17. Bartczak, Z.; Galeski, A.; Martuscelli, E.; Janik, H. Polymer 1985, 26, 1843.
18. Bartczak, Z.; Galeski, A.; Pracella, M. Polymer 1986, 27, 537.
19. Elms, W. J. Pop Plast 1987, 32, 32.
20. Mahajan, S. J.; Deopura, B. L.; Wang, Y. J Appl Polym Sci 1996, 60, 1517.
21. Quirk, R. P.; Alsamarraie, A. A. In Polymer Handbook; Immergut, E. H., Ed.; Wiley: New York, 1989; Vol. 5.
22. Buback, M.; Droge, T. Macromol Chem Phys 1997, 198, 3627.
23. Byun, H.-S.; Hasch, B. M.; McHugh, M. A.; Mahling, F.-O.; Busch, M.; Buback, M. Macromolecules 1996, 29, 1625.
24. Hasch, B. M.; Meilchen, M. A.; Lee, S.-H.; McHugh, M. A. J Polym Sci Part B Polym Phys 1992, 30, 1365.
25. Flory, P. J. Trans Faraday Soc 1955, 51, 848.
26. Brogly, M.; Nardin, M.; Schultz, J. J Appl Polym Sci 1997, 64, 1903.
27. Kim, Y. C.; Ahn, W.; Kim, C. Y. Polym Eng Sci 1997, 37, 1003.
28. Bouilloux, A.; Ernst, B.; Lobbrecht, A.; Muller, R. Polymer 1997, 38, 4775.
29. Kresge, E. N. In Polymer Blends; Newman, S., Ed.; Academic: New York, 1978; Vol. 2, p 293.
30. Gupta, A. K.; Ratnam, B. K.; Srinivasan, K. R. J Appl Polym Sci 1992, 45, 1303.